NASA TECHNICAL NOTE

SPECTRAL-AVERAGING ERROR REDUCTION IN LOW-RESOLUTION SPECTRORADIOMETRY

by Donald R. Buchele

Lewis Research Center
Cleveland, Ohio 44135

NATIONAL AERONAUTICS AND SPACE ADMINISTRATION • WASHINGTON, D. C. • FEBRUARY 1971

1. Report No.	2. Government Accession No.	3. Rec
NASA TN D-6131		

4. Title and Subtitle: SPECTRAL-AVERAGING ERROR REDUCTION IN LOW-RESOLUTION SPECTRORADIOMETRY

5. Report Date: February 1971

6. Performing Organization Code:

7. Author(s): Donald R. Buchele

8. Performing Organization Report No.: E-5271

9. Performing Organization Name and Address:
Lewis Research Center
National Aeronautics and Space Administration
Cleveland, Ohio 44135

10. Work Unit No.: 720-03

11. Contract or Grant No.:

12. Sponsoring Agency Name and Address:
National Aeronautics and Space Administration
Washington, D.C. 20546

13. Type of Report and Period Covered: Technical Note

14. Sponsoring Agency Code:

15. Supplementary Notes:

16. Abstract

Analytical methods are presented for reducing the error in the weighted average of a spectrally varying quantity when the weighting function is a spectrum measured by an instrument having low spectral resolution. The error is determined in terms of this resolution; this error increases as the resolution becomes lower. Spectroradiometers of the scanning type and the multiple-filter type are considered.

17. Key Words (Suggested by Author(s)):
Instrumentation; Optical techniques; Measurement, spectral; Spectroradiometry, low resolution; Resolution, spectral; Error reduction; Spectral analysis; Averaging, spectral; Radiometry, spectro-

18. Distribution Statement:
Unclassified - unlimited

19. Security Classif. (of this report)	20. Security Classif. (of this page)	21. No. of Pages	22. Price*
Unclassified	Unclassified	36	$3.00

*For sale by the National Technical Information Service, Springfield, Virginia 22151

CONTENTS

	Page
SUMMARY	1
INTRODUCTION	1
GENERAL ANALYSIS	2
Spread Function	3
Averaging Error	4
Relation Between Spread Function and Averaging Error	5
AVERAGING-ERROR REDUCTION BY COMPENSATION OF FOURIER TRANSFORM	7
Analysis	7
Example for a Scanning Spectroradiometer	10
FILTER RADIOMETER	12
Sampling and Interpolation with a Set of Equally Spaced Filters	12
Spread Function and Fourier Transform of a Set of Filters	14
Width and Spacing of Filters	15
Interpolation with a Finite Set of Unequally Spaced Filters	17
Example of Averaging-Error Reduction by Fourier-Transform Compensation	19
Assumed conditions	19
Random error due to sampling	19
Determination of compensating function	19
Error comparison	20
Optimum Filter Width for a Small Number of Equally Spaced Filters	22
AVERAGING-ERROR REDUCTION BY SPECTRAL-CURVE COMPENSATION	24
Analysis	24
Example for a Filter Radiometer	25
SUMMARY OF RESULTS	28
APPENDIXES	
A - SYMBOLS	29
B - CUBIC-SPLINE INTERPOLATION	31
REFERENCES	33

SPECTRAL-AVERAGING ERROR REDUCTION IN LOW-RESOLUTION SPECTRORADIOMETRY

by Donald R. Buchele

Lewis Research Center

SUMMARY

Analytical methods are presented for reducing the error in the weighted average of a spectrally varying quantity when the weighting function is a spectrum measured by an instrument having low spectral resolution. The error is determined in terms of this resolution; this error increases as the resolution becomes lower. Spectroradiometers of the scanning type and the multiple-filter type are considered.

INTRODUCTION

This report is directed to the improvement of the weighted average of a spectrally varying quantity when the weighting function is a spectrum measured by use of an instrument having low spectral resolution. The instrument may have one of two forms:

(1) A scanning spectroradiometer with a slit function of appreciable width

(2) A filter spectroradiometer using a discrete set of fixed filters, each of appreciable bandwidth

The analysis considers analytical techniques whereby the effective resolution of each of these instruments may be sharpened.

The mathematical treatment has wider applicability than just this problem. Thus, one may consider the weighted average Y of a spectrally varying quantity $y(\lambda)$ which is defined by

$$Y = \frac{\int_0^\infty N(\lambda)y(\lambda)d\lambda}{\int_0^\infty N(\lambda)d\lambda} \tag{1}$$

where $N(\lambda)$ is a weighting function, generally called the spectrum. (Symbols are defined in appendix A.) Typically, Y may be any of the following quantities: (1) emissivity, where $y(\lambda)$ is the spectral emissivity and $N(\lambda)$ is the spectral radiance of a blackbody at the surface temperature; (2) absorptivity, where $y(\lambda)$ is the spectral absorptivity of a surface and $N(\lambda)$ is the spectral radiance of incident radiation; (3) transmission factor, where $y(\lambda)$ is a spectral transmission factor of a material and $N(\lambda)$ is the spectral radiance of the radiation entering the material; or (4) detector sensitivity, where $y(\lambda)$ is the spectral sensitivity and $N(\lambda)$ is the spectral radiance of the incident radiation.

When $N(\lambda)$ is obtained by spectral radiometric measurements, it is known only with finite spectral resolution, which causes an error in the computed value of Y. It is often desirable to use a low-resolution spectral measurement, provided the resultant error in Y is small enough, because the low resolution and increased signal flux to the detector make possible a more favorable combination of signal-to-noise ratio and spectrum recording speed. Low resolution may be required to obtain enough signal flux for measurement. Instrument size and weight are often also reduced with low resolution.

This report determines the relation between spectral resolution and the error in Y. Analytical methods are then presented for reducing the error in Y. These methods also improve the spectral resolution, which may be useful in other applications of spectral measurement. The errors in Y caused by instrumental errors such as wavelength calibration and flux measurement will not be considered. The error due to flux measurement is reported by reference 1.

The analytical methods for error reduction are (1) compensation of the Fourier transform of the spread function and (2) spectral-curve compensation. Analogous examples of Fourier transform compensation are given in references 2 to 7. Applications of the technique of spectral-curve compensation are given in references 8 to 13. Fourier transform compensation will be treated first, because it is a general method applicable to both scanning spectroradiometers and filter radiometers. Then, the spectral-curve compensation method will be treated in its specific application to filter radiometers.

GENERAL ANALYSIS

This general analysis applies to both a scanning radiometer and a filter radiometer. However, a filter radiometer requires the further analysis given in the section FILTER RADIOMETER.

Spread Function

The transmission function of a filter or a spectrometer is given by

$$\tau(\nu) = \tau(\lambda - \lambda_i) \tag{2}$$

where λ_i is the nominal center wavelength of a filter, or a fixed wavelength setting of a spectrometer. Equation (2) is convenient for use in analysis; it assumes that $\tau(\nu)$ is the same at all values of λ_i. Measurement of $\tau(\nu)$ can be made in principle with a monochromatic source that sweeps across all wavelengths λ as λ_i remains constant.

As a result of finite spectral resolution, a spectral measurement $\overline{N}(\lambda_i)$ at a wavelength λ_i is then given by a cross-correlation integral (ref. 14) of $\tau(\nu)$ with the true spectrum $N(\lambda)$:

$$\overline{N}(\lambda_i) = \int_{-\infty}^{\infty} \tau(\nu) N(\lambda_i + \nu) d\nu \tag{3}$$

(For mathematical convenience, all integrals over a wavelength will have a lower limit of $-\infty$; although λ cannot physically become negative.)

Equation (3) can be transformed into a convolution integral (ref. 14)

$$\overline{N}(\lambda_i) = \int_{-\infty}^{\infty} g(\nu) N(\lambda_i - \nu) d\nu \tag{4}$$

where the transmission function $\tau(\nu)$ has been replaced by a spread function defined by

$$g(\nu) \equiv \tau(-\nu) \tag{5}$$

The spread function is the same as the transmission function only for even functions. The spread function of a filter is given conveniently by equation (5) after the transmission function has been measured. The spread function of a monochromator is conveniently measured by recording the spectrum of a monochromatic source fixed at λ_i.

The spectrum recorded by a scanning spectrometer is given by equation (4) when λ_i is continuously variable and replaced by λ so that

$$\overline{N}(\lambda) = \int_{-\infty}^{\infty} g(\nu) N(\lambda - \nu) d\nu \tag{6}$$

The spectrum measured by a filter radiometer is a set of readings, at $\lambda = \lambda_i$, given by equation (4) or (6); the readings are then interpolated to generate a spectral curve. Thus, the spectral curves produced by a scanning spectrometer and a filter radiometer agree only at λ_i, when both instruments have the same spread function.

A further simplification will be applied in some of the following sections by expanding equation (6) into a sum of two integrals

$$\overline{N}(\lambda) = \int_{-\infty}^{\infty} g_e(\nu)N(\lambda - \nu)d\nu + \int_{-\infty}^{\infty} g_o(\nu)N(\lambda - \nu)d\nu \tag{7}$$

where the spread function $g(\nu)$ is the sum of an even part $g_e(\nu)$ and an odd part $g_o(\nu)$. The odd part can be neglected, because (1) the functions generally found in practice are substantially even, and (2) the size of the odd integral can be made zero to a first-order approximation (ref. 2) by choosing the center wavelength λ_i of the spread function so that it is located at the centroid given by

$$\lambda_i = \frac{\int_{-\infty}^{\infty} \lambda g(\lambda)d\lambda}{\int_{-\infty}^{\infty} g(\lambda)d\lambda} \tag{8}$$

At this value of wavelength, a moderately asymmetrical spread function yields very nearly the same measurement of $\overline{N}(\lambda)$ as a symmetrical one.

Averaging Error

As a result of finite spectral resolution, the quantity computed from measurements is

$$\overline{Y} = \frac{\int_{-\infty}^{\infty} \overline{N}(\lambda)y(\lambda)d\lambda}{\int_{-\infty}^{\infty} \overline{N}(\lambda)d\lambda} \tag{9}$$

where the result of finite-resolution measurements is designated by a bar. The error made in determination of Y is

$$\overline{Y} - Y = \frac{\int_{-\infty}^{\infty} \overline{N}y\, d\lambda}{\int_{-\infty}^{\infty} \overline{N}\, d\lambda} - \frac{\int_{-\infty}^{\infty} Ny\, d\lambda}{\int_{-\infty}^{\infty} N\, d\lambda} \tag{10}$$

A useful equality (ref. 14) of the convolution integral, equations (4) and (6), (which also holds for the cross-correlation integral, eq. (3)) is

$$\int_{-\infty}^{\infty} \overline{N}\, d\lambda = \int_{-\infty}^{\infty} g\, d\nu \cdot \int_{-\infty}^{\infty} N\, d\lambda \tag{11}$$

Combining equations (1), (10), and (11) yields the fractional error

$$\frac{\Delta Y}{Y} = \frac{\int_{-\infty}^{\infty} (A\overline{N} - N)y\, d\lambda}{\int_{-\infty}^{\infty} Ny\, d\lambda} \tag{12}$$

where

$$A = \frac{1}{\int_{-\infty}^{\infty} g\, d\nu} \tag{13}$$

Relation Between Spread Function and Averaging Error

Substituting equation (6) into equation (12) and exchanging the order of integration yields

$$\frac{\Delta Y}{Y} = \frac{A \int_{-\infty}^{\infty} h(\nu)g(\nu)d\nu}{\int_{-\infty}^{\infty} N(\lambda)y(\lambda)d\lambda} - 1 \tag{14}$$

where $h(\nu)$ is a cross-correlation integral

$$h(\nu) = \int_{-\infty}^{\infty} y(\lambda)N(\lambda - \nu)d\lambda \tag{15}$$

The denominator appearing in equation (14) is

$$h(0) = \int_{-\infty}^{\infty} N(\lambda)y(\lambda)d\lambda \tag{16}$$

When $g(\nu)$ is a unit-area impulse $\delta(\nu)$ representing infinite spectral resolution, the integral in the numerator of equation (14) becomes $h(0)$, and the error is zero.

When equation (16) is substituted in (14), the error is

$$\frac{\Delta Y}{Y} = \frac{A \int_{-\infty}^{\infty} h(\nu)g(\nu)d\nu}{h(0)} - 1 \qquad (17)$$

If $g(\nu)$ is an even function and lies entirely within a strictly linear range of $h(\nu)$, the error is zero.

Although both equations (12) and (17) can be used to compute the error, equation (17) explicitly shows the relation between the spread function (or spectral resolution) and the error. Equation (17) provides the means for determining how much $g(\nu)$ should be narrowed, or be made more symmetrical about $\nu = 0$, should the first computation of $|\Delta Y/Y|$ show this quantity to be excessive.

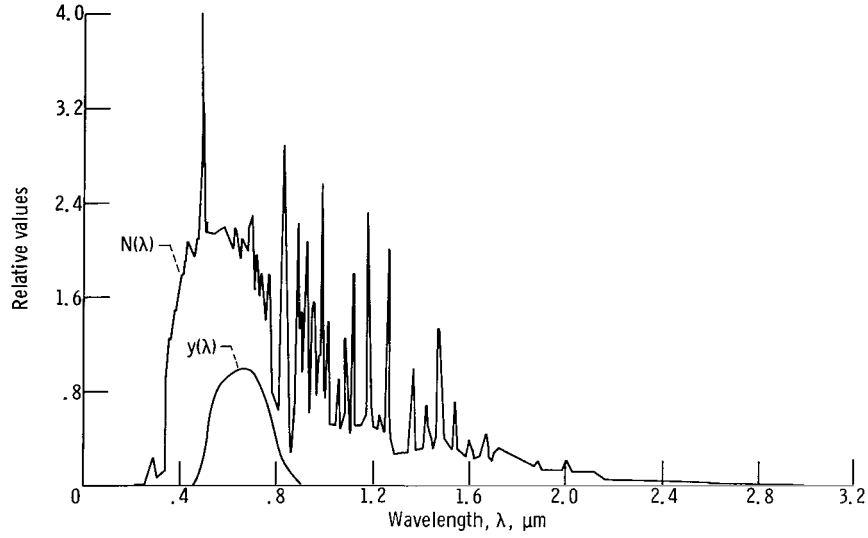

(a) Plot with N and y given.

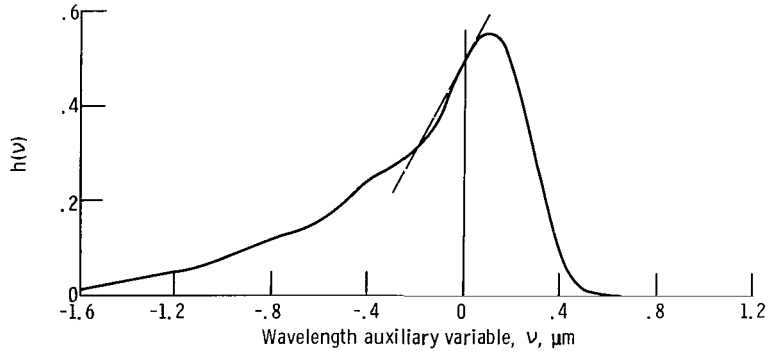

(b) Cross correlation of N and y.

Figure 1. - Determination of spread-function width.

The spread function width that will yield an acceptably small error, yet be as wide as possible, can be established in the following steps (these steps will be illustrated by the parallel example of fig. 1):

(1) Given a spectrum $N(\lambda)$ and a detector having response $y(\lambda)$ (e.g., the xenon spectrum and the cadmium-sulphide photosurface sensitivity shown in fig. 1(a)), compute the cross-correlation function $h(\nu)$, equation (15) (fig. 1(b) for the example).

(2) Determine a range of ν about $\nu = 0$ at which the separation of $h(\nu)$ from a tangent line at $\nu = 0$ does not exceed the specified error (see fig. 1(b)).

(3) Select a spread function half-maximum width that is within the selected range of ν, and compute the error with equation (17). If the maximum error thus computed is too large or too small, select another width and recompute the error.

AVERAGING-ERROR REDUCTION BY COMPENSATION OF FOURIER TRANSFORM

Analysis

The purposes of this section are to find the effective spread function shape produced by Fourier transform compensation and to illustrate a simple type of compensation. When an effectively even function $g(\nu) = g_e(\nu)$ is assumed and the convolution symbol * is used, equation (6) becomes

$$\overline{N}(\lambda) = g_e(\lambda) * N(\lambda) \tag{18}$$

which has a transform

$$\overline{\mathcal{N}}(s) = \mathcal{G}_e(s)\mathcal{N}(s) \tag{19}$$

The shape of the spread function can be compensated to yield an effectively higher resolution by multiplying its transform $\mathcal{G}_e(s)$ with a compensating function $\mathcal{F}_C(s)$ so that $\mathcal{F}_C(s)\mathcal{G}_e(s) \approx$ constant over some range of s about $s = 0$. Full compensation ($\mathcal{F}_C(s)\mathcal{G}_e(s) =$ constant for all s) is not practical at values of s where $\mathcal{G}_e(s) \approx 0$ because measurement error is magnified by compensation (ref. 15). With the corresponding compensating function $f_C(\nu)$, equations (18) and (19) become, respectively,

$$f_C(\lambda) * \overline{N}(\lambda) = f_C(\lambda) * g_e(\lambda) * N(\lambda) \tag{20}$$

$$\mathcal{F}_C(s)\overline{\mathcal{N}}(s) = \mathcal{F}_C(s)\mathcal{G}_e(s)\mathcal{N}(s) \tag{21}$$

Thus, the compensated spread function may be computed with the convolution

$g_C(\lambda) = f_C(\lambda) * g_e(\lambda)$ (in order to observe the nature of the improvement). The corrected spectrum can be computed with the convolution $f_C(\lambda) * \overline{N}(\lambda)$. References 4 and 5 specify $\mathcal{F}_C(s)\mathcal{G}_e(s)$ for a particular application. References 6 and 7 specify $\mathcal{F}_C(s)$ using a criterion of minimum least square error of the difference $\overline{N}(\lambda) - N(\lambda)$, thus automatically avoiding excessive magnification of the measurement error.

Reference 3 compensated $\mathcal{G}_e(s)$ with a trigonometric polynomial which lends itself to simple numerical computation. It will now be applied to demonstrate the change in spread-function shape after compensation. For an even spread function $g_e(\nu)$, the first-order trigonometric correction term is also an even function, and thus real, given by

$$\mathcal{F}_C(s) = 1 + b \sin^2 \pi a s = 1 + (b/2)(1 - \cos 2\pi a s) \tag{22}$$

where the constants b and a are constrained to make $\mathcal{F}_C(s)\mathcal{G}_e(s) \approx$ constant for small values of s. This constraint is satisfied by use of the moment theorem (refs. 14 and 16) (the second moment of the spread function is proportional to the second derivative of its transform at $s = 0$), which leads to

$$ba^2 = 2\sigma^2 \tag{23}$$

where σ is the standard deviation of the spread function and is given by

$$\sigma^2 \equiv \frac{\int_{-\infty}^{\infty} \nu^2 g_e(\nu) d\nu}{\int_{-\infty}^{\infty} g_e(\nu) d\nu} \tag{24}$$

A value of $a = \sigma$ in equation (23) is suggested by reference 3, which gives $b = 2$. If the spread function has a value of σ that is very large or infinite, a graphical method of selecting a and b must be used (ref. 3). Equation (22) and its inverse transform to the ν domain are shown in figure 2.

Fourier transform compensation will now be applied, with $a = \sigma$ and $b = 2$ for the compensating function. Examples of Gaussian and rectangular spread functions and their transforms are shown in figures 3 and 4, together with the compensating function $\mathcal{F}_C(s)$ and its inverse transform. The large negative values in the compensated function $\mathcal{G}_C(s)$ of figure 4(c) may be reduced by use of a different value of a such as $a = 2\sigma$, giving $b = 0.5$ by equation (23). After compensation, the standard deviation of the spread function always has an undesirable increase because of the convolution $f(\nu) * g_e(\nu)$. However, the shape of the altered spread function in these examples has negative values at the wings, so that there is an overall improvement. When this spread function is integrated in equation (17), the negative values tend to reduce the error.

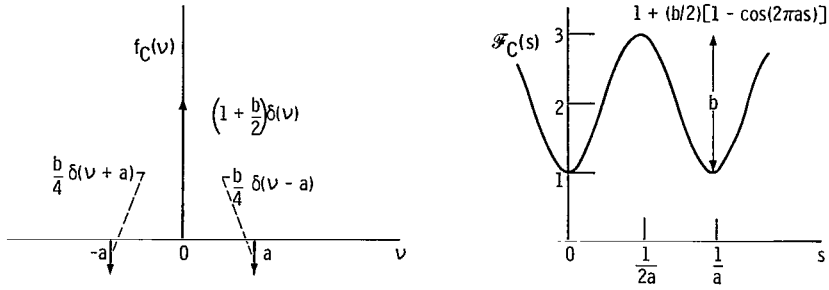

(a) Inverse transform of compensating function.

(b) Compensating function.

Figure 2. - First-order term of trigonometric polynomial compensating function.

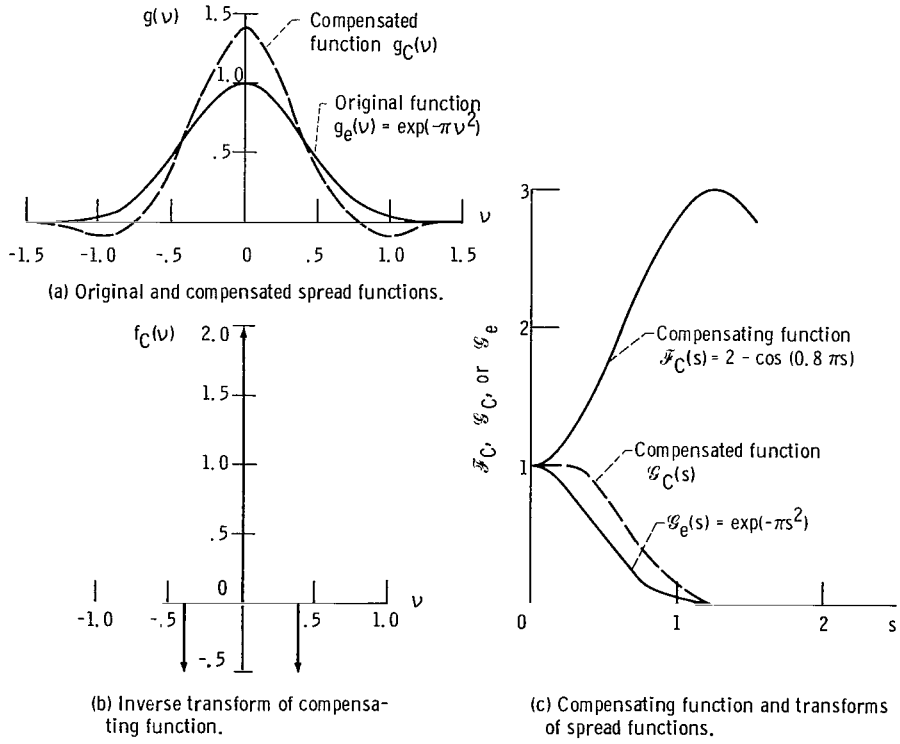

(a) Original and compensated spread functions.

(b) Inverse transform of compensating function.

(c) Compensating function and transforms of spread functions.

Figure 3. - Example of Gaussian spread function, with standard deviation $\sigma = 0.4$, compensated by trigonometric polynomial with constants of function $\mathcal{F}_C(s)$ being $a = \sigma$ and $b = 2$.

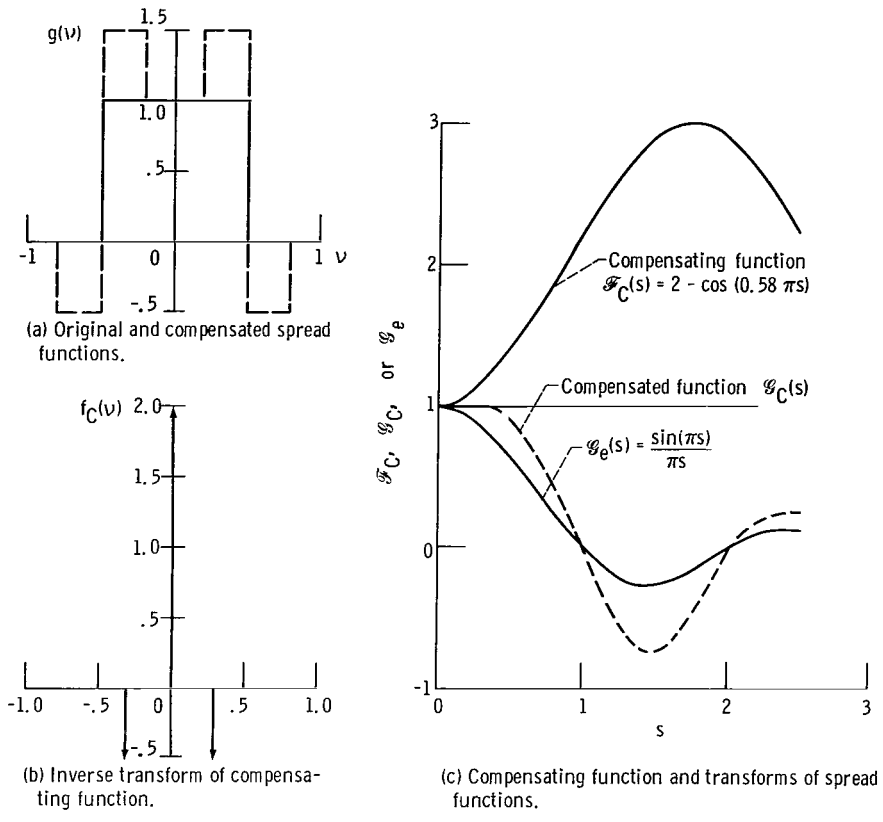

(a) Original and compensated spread functions.

(b) Inverse transform of compensating function.

(c) Compensating function and transforms of spread functions.

Figure 4. - Example of rectangular spread function, with standard deviation $\sigma = 0.29$, compensated by trigonometrical polynomial with constants of function $\mathscr{F}_C(s)$ being $a = \sigma$ and $b = 2$.

Example for a Scanning Spectroradiometer

The averaging error will be computed for the xenon-arc lamp spectrum and the cadmium sulfide photosurface shown in figure 1(a). The cross correlation of these curves is $h(\nu)$, shown in figure 1(b). The spread function that will be assumed for the spectrometer is

$$g_e = 1 + \cos(\pi\nu/w), \qquad |\nu/w| \leq 1 \tag{25}$$

where w is the half-maximum width of $g_e(\nu)$. This function is shown in figure 5(a). The error computed with equations (12) and (17) is plotted in figure 5(c). Both equations give the same error.

Analytical reduction of the error used the compensating function of equation (22). A value of $a = \sigma$ was used in equation (23) as suggested by reference 3, giving $b = 2$. Thus, the ordinates of the compensating function $f_C(\nu)$ in figure 2 become -0.5 and 2.0

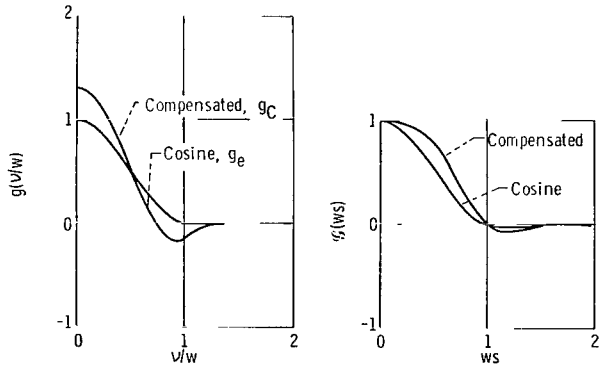

(a) Spread function of spectroradiometer.

(b) Transform.

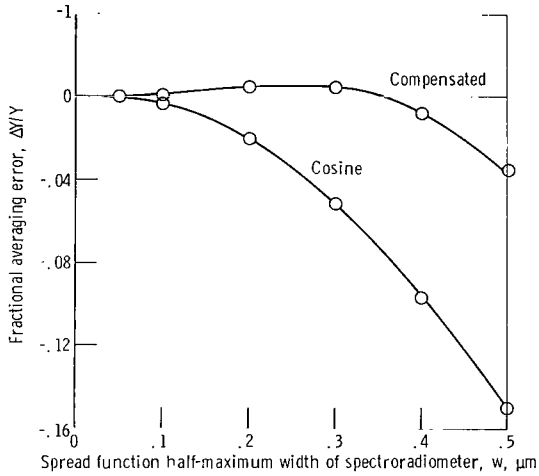

(c) Averaging error (curves from eq. (12); points from eq. (17)

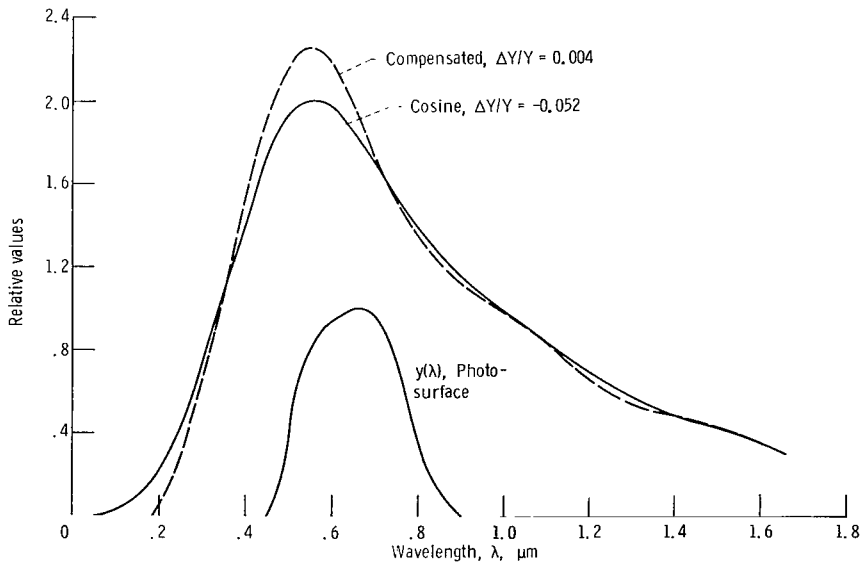

(d) Xenon spectrum; half-maximum width of spread function = 0.3.

Figure 5. - Scanning spectroradiometer with Fourier-transform compensation.

with $a = \sigma_e = 0.36$ w for the spread function $g_e(\nu)$. Convolution of $f_C(\nu)$ with $g_e(\nu)$ produced the compensated function $g_C(\nu)$, shown in figure 5(a) for comparison with $g_e(\nu)$. The corresponding transforms are shown in figure 5(b), and the spectra are shown in figure 5(d). The averaging error, plotted in figure 5(c) as a function of spectral resolution, has been substantially reduced. An error of 5 percent at 0.3 micrometer was reduced to 0.5 percent. Conversely, for a given 0.5 percent error, the spread function could be three times wider if analytical error reduction were to be applied subsequent to the measurement.

This example illustrates that the averaging error need not be large when the spectrum consists of many emission lines rather than being a smooth curve. The spectral measurement does not have to resolve an emission line. It is generally adequate to have the spectral width of the spread function $g(\nu)$ less than the spectral width of either $N(\lambda)$ or $y(\lambda)$, whichever one has the greater width. This is shown more precisely by equation (17), where the error becomes small when the spectral width of $g(\nu)$ is less than that of $h(\nu)$, and $h(\nu)$ is the cross correlation of $N(\lambda)$ with $y(\lambda)$. In the present example, the half-maximum width of $y(\lambda)$ was 0.27 micrometer. An averaging error of 0.5 percent was produced with a half-maximum width $g_e(\nu)$ of 0.12 micrometer, which is one-half the half-width of $y(\lambda)$; if subsequent analytical compensation were to be used, the half-width of $g_e(\nu)$ could be 0.38 micrometer, which is approximately equal to the 0.27-micrometer half-width of $y(\lambda)$. Thus, a small averaging error can be obtained with rather wide spread functions.

FILTER RADIOMETER

Sampling and Interpolation with a Set of Equally Spaced Filters

The spectrum obtained with an infinite set of equally spaced symmetrical filters is the result of three steps:

(1) When a spread function of a filter scans the spectrum continuously, the resultant measured spectrum $\overline{N}(\lambda)$, expressed by equation (6) or (18), represents a smoothing of the original spectrum $N(\lambda)$.

(2) If, now, the form of the spread function is fixed and repeated at center wavelengths λ_i spaced at intervals $\Lambda = \lambda_{i+1} - \lambda_i$, it represents a set of filters. Radiation measurement with each filter is a sample of $\overline{N}(\lambda)$ at $\lambda = \lambda_i$. The samples are

$$\overline{N}(\lambda_i) = \overline{N}(\lambda_0 + i\Lambda), \; i = -\infty, \ldots, 0, 1, \ldots, \infty \tag{26}$$

where λ_0 is the center wavelength of one of the filters. The samples are periodically

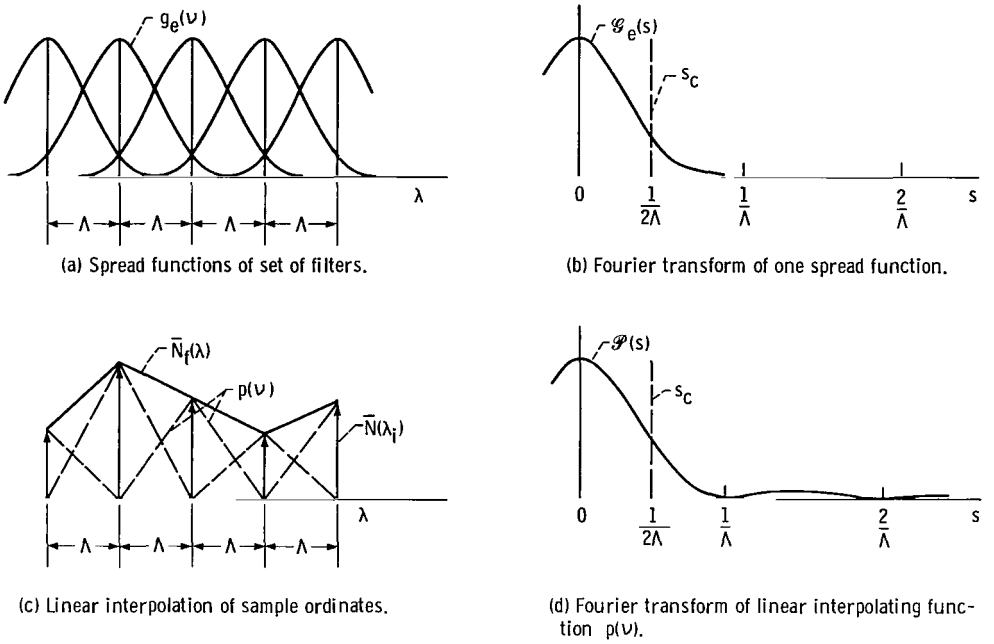

(a) Spread functions of set of filters.

(b) Fourier transform of one spread function.

(c) Linear interpolation of sample ordinates.

(d) Fourier transform of linear interpolating function $p(\nu)$.

Figure 6. - Sampling and interpolation with set of filters.

reproduced, as multiples of Λ are added to λ_0. Figure 6(a) shows some spread functions $g_e(\nu)$ spaced at an interval Λ; figure 6(b) shows the Fourier transform $\mathcal{G}_e(s)$ of one spread function.

(3) A spectral curve is generated by fitting a curve through the sample ordinates $\bar{N}(\lambda_i)$. The curve-fitting method commonly used in Fourier transform analysis is the convolution of an interpolating function $p(\nu)$ with equally spaced sample ordinates $\bar{N}(\lambda_i)$. The convolution integral reduces to a summation, giving a spectral curve designated by the subscript f:

$$\bar{N}_f(\lambda) = \sum_{i=-\infty}^{\infty} \bar{N}(\lambda_i)p(\nu) \tag{27}$$

Figure 6(c) shows ordinates $\bar{N}(\lambda_i)$ with triangular (linear) interpolating functions $p(\nu)$. Figure 6(d) shows the transform $\mathcal{P}(s)$ of $p(\nu)$.

Summarizing, the three steps are (1) smoothing of $N(\lambda)$ by $g_e(\nu)$ to produce $\bar{N}(\lambda)$, (2) sampling of $\bar{N}(\lambda)$ at intervals Λ to produce $\bar{N}(\lambda_i)$ and (3) interpolation of $\bar{N}(\lambda_i)$ by $p(\nu)$ to produce $\bar{N}_f(\lambda)$.

The dashed vertical line in figure 6(b) corresponds to the interval Λ, and its abscissa $s_c = 1/(2\Lambda)$ is the "sampling cutoff frequency." Values of s to the right and to the left of s_c have different effects.

Values of s to the right of s_c correspond to sinusoidal components, in the wavelength spectrum $N(\lambda)$, with a period less than 2Λ. These short-period components of $N(\lambda)$ are substantially attenuated by the inverse transform of $\mathscr{g}_e(s)$ and then become components of $\overline{N}(\lambda)$. The short-period components of $\overline{N}(\lambda)$ are then sampled at an interval Λ that is greater than one-half their period; they therefore cannot be reconstituted from the sampled data; they become an error of different period (called "aliasing" error) in the reconstituted spectrum $\overline{N}_f(\lambda)$. The error at any wavelength depends on the arbitrary value of λ_0 in equation (26). This limitation is a result of the sampling theorem (ref. 14).

Values of s to the left of s_c correspond to sinusoidal components, in the wavelength spectrum $N(\lambda)$, with a period greater than 2Λ. The long-period components of $N(\lambda)$ are attenuated by the inverse transform of $\mathscr{g}_e(s)$ to become components of $\overline{N}(\lambda)$. These long-period components of $\overline{N}(\lambda)$ are then sampled at an interval less than one-half their period; they therefore can be reconstituted in their attenuated form from sampled data, as proved by the sampling theorem (ref. 14). With interpolation between wavelengths λ_i, these long-period components of $\overline{N}(\lambda)$ can be further attenuated by the inverse transform of $\mathscr{P}(s)$ to become components of $\overline{N}_f(\lambda)$ (eq. (27)). Thus, the combined effect of the spread function and of interpolation is to attenuate the long-period components of $N(\lambda)$ by the inverse transform of product $\mathscr{g}_e(s)\mathscr{P}(s)$. This attenuation can be compensated for values of $|s| < s_c$ by either of the two general methods of reducing averaging error. Thereby, the long-period components of $N(\lambda)$ can be reconstituted.

Attenuation by the interpolating function can be avoided by use of a $\operatorname{sinc}(\pi\nu/\Lambda)$ interpolating function defined by

$$p(\nu) = \operatorname{sinc}(\pi\nu/\Lambda) \equiv \sin(\pi\nu/\Lambda)/(\pi\nu/\Lambda) \tag{28}$$

which has a transform that is constant for $|s| \leq 1/(2\Lambda)$ and zero elsewhere. This function is useful in analysis, but it has practical limitations. An alternative interpolating function is recommended in the section Interpolation with a Finite Set of Unequally Spaced Filters.

In the following sections the quantities $\mathscr{g}_e(s)$, $\mathscr{P}(s)$, and s_c will be related to the spread-function shape corresponding to a set of filters and to the choice of filter spacing Λ.

Spread Function and Fourier Transform of a Set of Filters

The effective spread function g_f for each filter in a set of fixed filters differs from the spread function g_e for the same filter when it is used in a continuous scan mode,

because of sampling and interpolation. The effect of sampling is to add the ordinarily random aliasing error

$$\mathcal{N}(s)\mathcal{G}_e(s) \quad \text{for } |s| > s_c$$

to

$$\mathcal{N}(s)\mathcal{G}_e(s) \quad \text{for } |s| \leq s_c$$

This random aliasing error may be neglected in attempting to determine and correct for the averaging error.

The effect of interpolation is to attenuate $\mathcal{N}(s)\mathcal{G}_e(s)$ for $|s| < s_c$ by a factor $\mathcal{P}(s)$. Thus, the spread function for a set of fixed filters has a transform given by

$$\begin{aligned} \mathcal{G}_f(s) &= \mathcal{G}_e(s)\mathcal{P}(s) \qquad |s| \leq s_c \\ \mathcal{G}_f(s) &= 0 \qquad\qquad\quad |s| > s_c \end{aligned} \tag{29}$$

that includes the effect of sampling and interpolation on $\mathcal{G}_e(s)$. The corresponding spread function $g_f(\nu)$ for a set of filters is the convolution

$$g_f(\nu) = g_e(\nu) * p(\nu) * \operatorname{sinc}(\pi\nu/\Lambda) \tag{30}$$

where the truncation at s_c is produced by $\operatorname{sinc}(\pi\nu/\Lambda)$. Equation (30) shows that $g_f(\nu)$ is wider than $g_e(\nu)$.

Width and Spacing of Filters

The requirement that the maximum fractional error $\Delta Y/Y$ be less than a specified amount imposes restrictions (1) on the width of the filters and (2) on the spacing of the filters. The recommended criteria for width and spacing are

(1) The spread function of the filter should be the $g_f(\nu)$ of equation (29) or (30), and its width should be selected as indicated in the section Relation Between Spread Function and Error.

(2) For the filter width selected in criterion (1), the filter spacing should be close to twice the standard deviation σ, equation (24), of the spread function of the filter $g_e(\nu)$.

The result of satisfying criterion (2) is illustrated in figure 7, which shows rectangular, triangular, and Gaussian functions with a separation $\Lambda = 2\sigma$. These functions

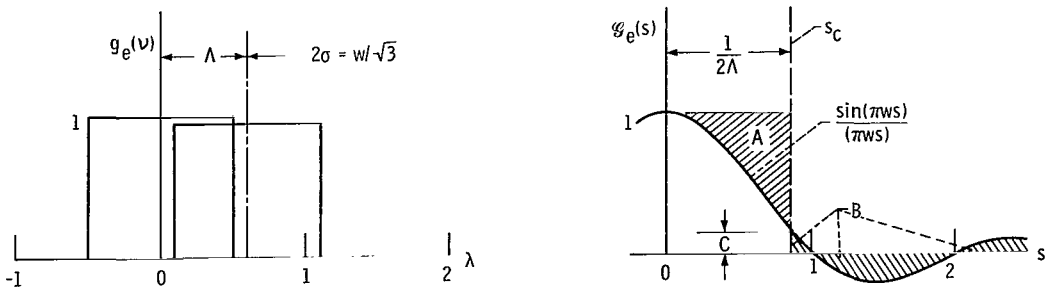

(a) Rectangular filter function.

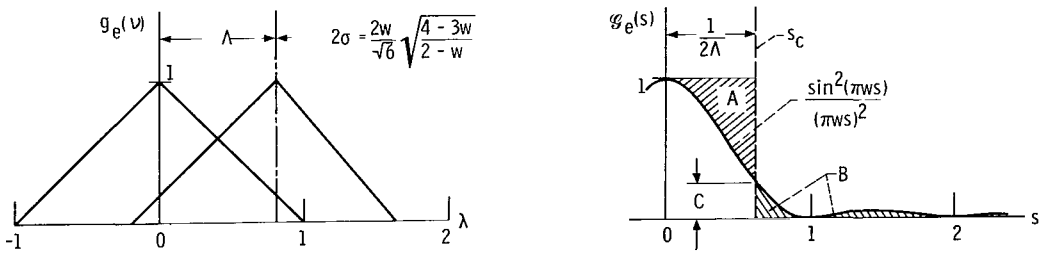

(b) Triangular filter function.

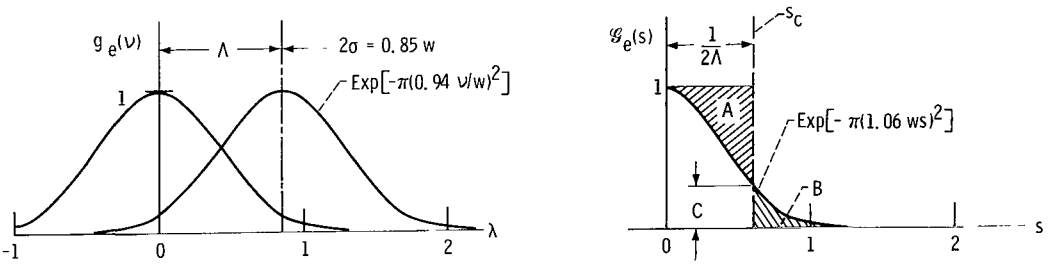

(c) Gaussian filter function.

Figure 7. - Filter separation and Fourier transform of one filter. Half-maximum width of spread function = 1.

represent filters found in practice that range from rectangular to triangular to Gaussian in shape. The Fourier transform $\mathcal{G}_e(s)$ is shown for each case. The abscissa of the dashed vertical line in the transform plane is the "sampling cutoff frequency," $s_c = 1/(2\Lambda)$. This vertical line has the following significance:

(1) Area A to the left of the line represents a correctable attenuation of long-period sinusoidal components in the spectrum $N(\lambda)$.

(2) Area B to the right of the line represents attenuated short-period components in the spectrum $N(\lambda)$, which, after sampling, produce an uncorrectable error in the reconstituted spectrum $\overline{N}_f(\lambda)$. For the scanning radiometer, area A extends to infinity, and area B is zero, because the sampling interval Λ is zero, and s_c becomes infinite.

(3) The location of the line represents a compromise between several considerations: The correction for attenuation, area A, utilizes division by the ordinates of the curve up to s_c; as the vertical line is moved to the right, the distance C must not be allowed to become too small because measurement error for sinusoidal components of $\overline{N}(\lambda)$ with a short period near to 2Λ would be magnified excessively (ref. 15). On the other hand, as the vertical line is moved to the left, area B increases rapidly, giving an undesirable increase in the uncorrectable error caused by sampling.

Thus, the filter separation Λ must be such as to minimize the sum of variances represented by areas A and B. The compromise spacing $\Lambda = 2\sigma$ makes $C = 0.15$ for the rectangular function, $C = 0.24$ for the triangular function, and $C = 0.29$ for the Gaussian function. The functions $g_e(\nu)$ show substantial overlapping with this spacing.

Interpolation with a Finite Set of Unequally Spaced Filters

The ideal band-limited interpolation with a $\mathrm{sinc}(\pi\nu/\Lambda)$ function is not recommended because of the following conditions:

(1) Filter center wavelengths are unequally spaced. Nominally equal spacing is not easily obtained, because of fabrication tolerances. Furthermore, the spacing is often progressively increased with wavelength to maintain a constant ratio of spacing to wavelength.

(2) The set of filters is finite. An interpolation error arises from lack of readings that would be provided by nonexistent filters outside the set. These readings would contribute to interpolation within the set through the slowly decaying sinc interpolating function. This error has been considered by references 17 and 18. Attempts have been made to minimize this error by the use of more rapidly decaying interpolation functions (refs. 19 and 20).

(3) Extrapolation beyond the first and last filter center wavelengths is necessary to apply the methods of averaging-error reduction.

(4) Negative values of radiation are not permitted.

Cubic spline interpolation (ref. 21) is appropriate for overcoming the first three objections. It is described in appendix B. A function $p(\nu)$ (eq. (27)) that approximates cubic-spline interpolation and that is more convenient for analytical treatment of equally spaced intervals is

$$p(\nu) = 0.4 \sin(\pi\nu/\Lambda)/\sinh(0.4\,\pi\nu/\Lambda) \tag{31}$$

The approximation is within 1 percent everywhere except very near to λ_1 and to λ_n. This function is shown in figure 8(a). For comparison, the $\mathrm{sinc}(\pi\nu/\Lambda)$ function, equa-

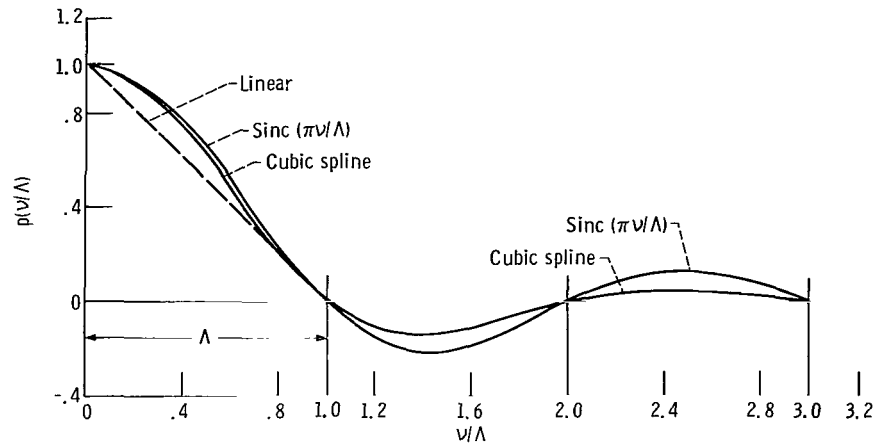

(a) Interpolating function.

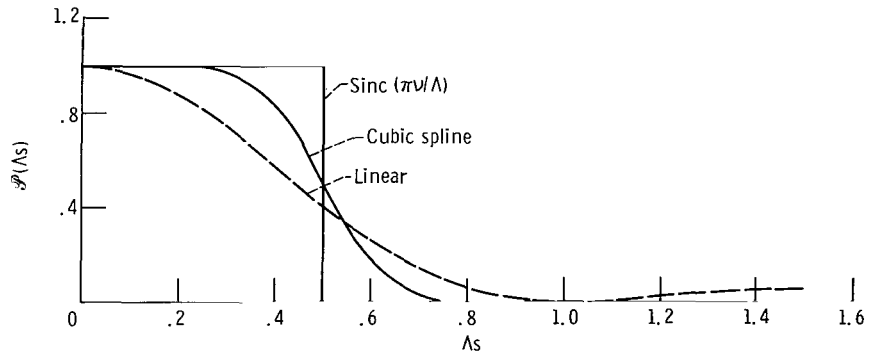

(b) Fourier transform.

Figure 8. - Interpolating function and its transform.

tion (28), and a linear function are also plotted. The spline function has a faster decay, desirable for condition (2).

The transform of equation (31), shown in figure 8(b), is

$$\mathscr{P}(s) = \Lambda \sinh(2.5\,\pi)/(\cosh 2.5\,\pi + \cosh 5\pi s\Lambda) \tag{32}$$

This curve is intermediate between the linear and the sinc function transforms.

At the first and last filter center wavelengths, λ_1 and λ_n, the cubic spline computed with equation (B1) has zero curvature. Linear extrapolation of the slope given by the derivative of equation (B1) is appropriate for condition (3).

The negative values of radiation sometimes produced by interpolation or extrapolation are replaced by zero to satisfy condition (4). However, during averaging-error reduction by the method of spectral curve compensation, to be treater later, it was found desirable to retain negative values for iterative adjustment of their magnitude and to replace negative values by zero just before integrating the product of spectral radiation by the spread function.

Example of Averaging-Error Reduction by Fourier-Transform Compensation

Assumed conditions. - The averaging error was computed for the same xenon source, cadmium sulfide photosurface, cosine spread function (eq. (25)), and method of error reduction as used in the earlier example with a scanning spectroradiometer. The spread functions were spaced by the recommended 2σ so that $\Lambda = 2\sigma = 0.72$ w.

Random error due to sampling. - To obtain a value for the random error due to sampling by a given set of filters, four spectral curves were determined for that set, as the entire set was shifted, relative to the spectrum, by successive wavelength displacements of $\Lambda/4$, $\Lambda/2$, and $3\Lambda/4$ from an initial position. Four typical spectral curves are shown in figure 9 for the case of five filters having w = 0.3 micrometer.

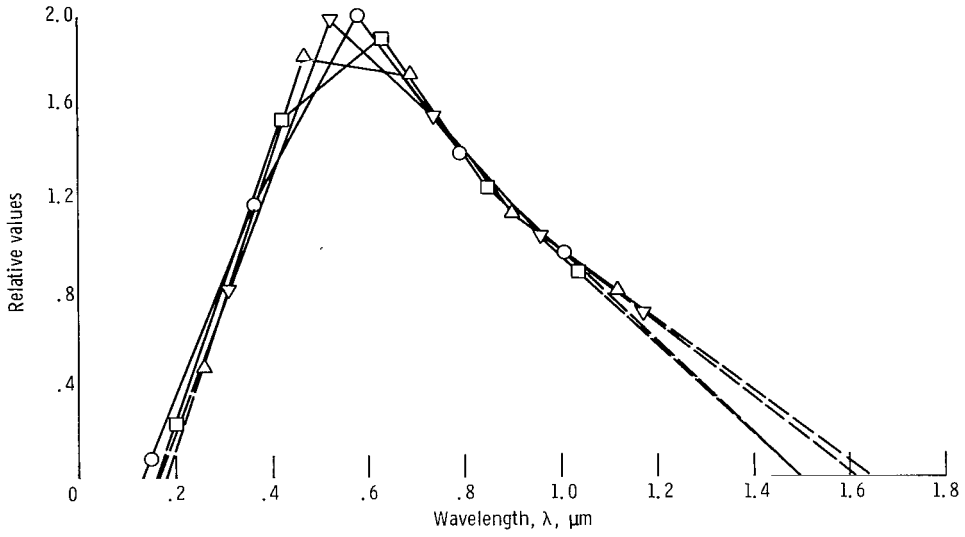

Figure 9. - Xenon spectra with linear interpolation between readings of five filters of half-maximum width of 0.3 micrometer, spaced by 0.216 micrometer. Each filter in set is displaced in three steps of 0.054 micrometer to generate four curves.

The averaging error was computed for each curve using equation (12). The average deviation from the mean of these four averaging errors is the random error due to sampling.

Determination of compensating function. - Error reduction used the compensating function of equation (22), where the constants a and b were constrained by

$$\mathcal{F}_C(s)\mathcal{G}_f(s) = \mathcal{F}_C(s)\mathcal{G}_e(s)\mathcal{P}(s) \approx \text{constant}$$

for small values of s. We define

$$\sigma_f^2 = \sigma_e^2 + \sigma_p^2$$

and choose $a = \sigma_f$ as suggested by reference 3. Applying the moment theorem (ref. 14), we have

$$4\pi^2\sigma_e^2 = -\mathscr{G}_e''(0)$$

$$4\pi^2\sigma_p^2 = -\mathscr{P}''(0)$$

and note that

$$\mathscr{G}_e''(0) \approx -5.2\ w^2$$

for the spread function,

$$\mathscr{P}''(0) = 0$$

for the cubic spline, and

$$\mathscr{P}''(0) = -2\pi^2\Lambda^2/3$$

for the linear interpolating function. Adopting the recommendation given in the section Width and Spacing of Filters that

$$\sigma_e = \Lambda/2$$

leads to

$$a = 0.36\ w$$

for cubic spline interpolation and

$$a = 0.47\ w$$

for linear interpolation. The second value of a provides the extra compensation required by linear interpolation.

Error comparison. - The errors before and after compensation are plotted in figures 10(a) and 11(a). An extra curve is shown in figure 10(a) for $a = 0.36\ w$ to show the partial compensation when the effect of interpolation is neglected in choosing the value of a. Comparing these curves to the scanning spectroradiometer curves in fig-

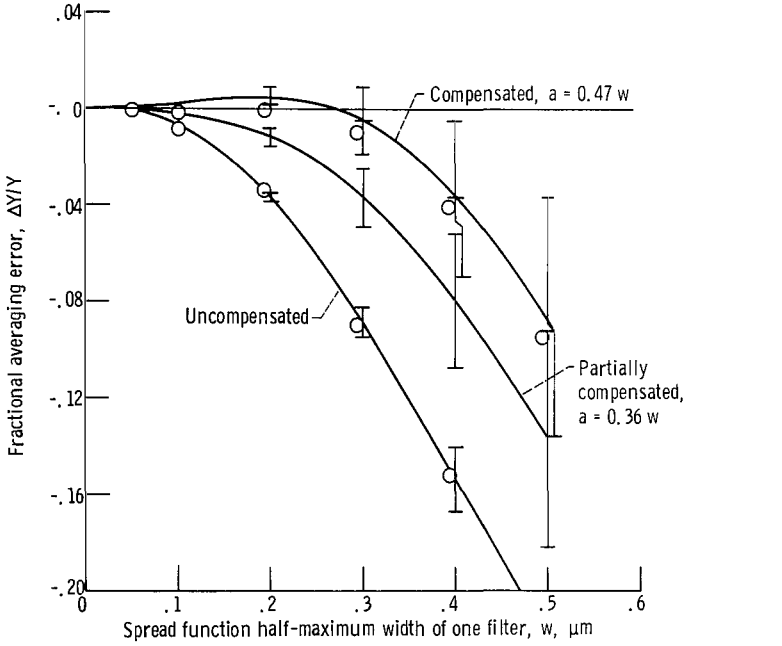

(a) Averaging error (curves from eq. (12) (bars are average deviation); points from eq. (17)).

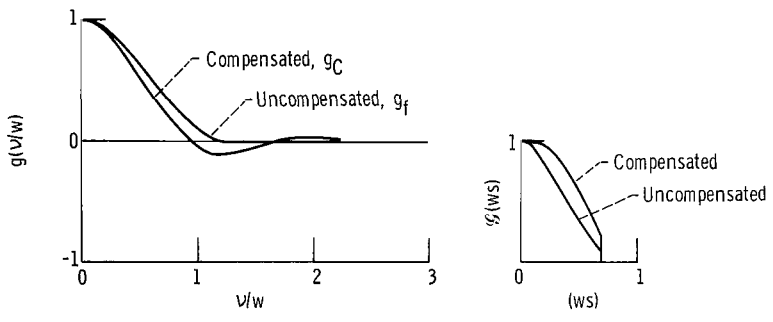

(b) Spread function of set of filters. (c) Transform.

Figure 10. - Filter radiometer with linear interpolation and Fourier transform compensation.

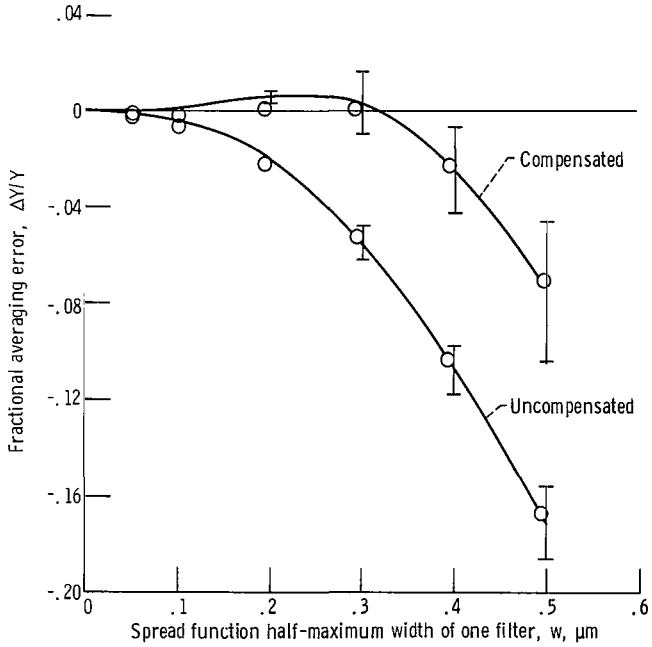

(a) Averaging error (curves from eq. (12) (bars are average deviation); points from eq. (17)).

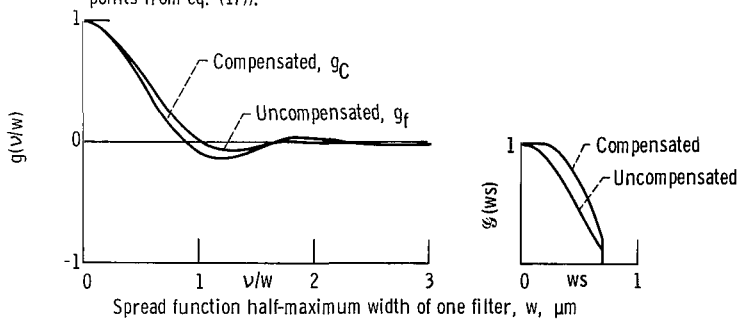

(b) Spread function of set of filters. (c) Transform.

Figure 11. - Filter radiometer with spline interpolation and Fourier transform compensation.

ure 5 shows that the averaging error after compensation, for $w < 0.3$, is effectively the same for both instruments. Figures 10 and 11 also show the random errors (average deviations) caused by sampling. The average deviation is doubled after correction, and it is then comparable to the averaging error. The average deviation is greater for linear interpolation than for spline interpolation.

The spread functions and transforms, shown in figures 10(b), 10(c), 11(b), and 11(c), are substantially different from those of figures 5(a) and (b).

Optimum Filter Width for a Small Number of Equally Spaced Filters

The illustrative examples have assumed that the number of filters used was so large that an increase in their number would not produce a significant decrease in the final errors. For some space applications, where mass or bulk of the instruments is of great significance, one may want to examine the effects of using a very small number of filters. This section considers this problem; specifically, the final errors associated with using three to seven filters.

For a given spectrum to be analyzed, and a given number of filters, there will be some value of w, the half-maximum filter width, which minimizes the systematic error after compensation, the random error due to sampling, or any chosen combination of these two errors, such as the sum of the systematic and random variances. This situation is in contrast to the case where the number of filters is large, because then the errors always decrease as w decreases.

For concreteness, the problem to be treated will be confined specifically to the same source, detector, and filter spread function used in the previous examples and will assume cubic-spline interpolation. The results are plotted in figure 12 for filters that were symmetrically placed over the cadmium sulfide response band of 0.45 to 0.9 micrometer. Using the criterion of minimum sum of systematic and random variances, one result is that the total variance is a minimum, or close to a minimum, for $w \approx 0.25$ micrometer, regardless of the number of filters. Another result is that, on the locus of minimum variance, four filters have a wavelength span 50 percent greater than the 0.45-micrometer span of the detector. As the number of filters increases, the wavelength span of the filters approaches that of the detector. In this example, there is little advantage to using more than four filters.

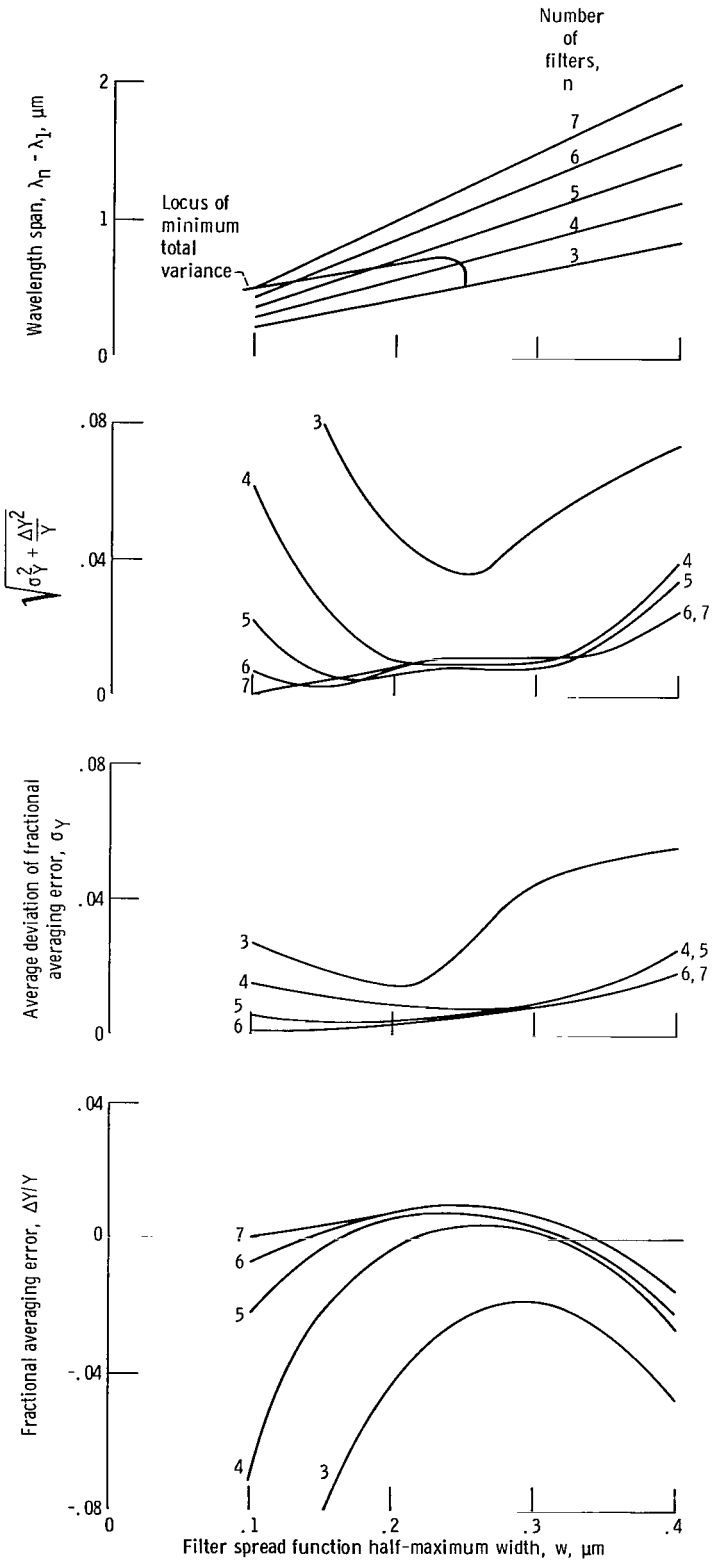

Figure 12. - Error dependence on number of filters and width of filter.

AVERAGING-ERROR REDUCTION BY SPECTRAL-CURVE COMPENSATION

Analysis

After readings have been taken with a set of filters, a low-resolution spectral curve is drawn by interpolation between the readings when these have been plotted at the center wavelengths of the filters. Using this low-resolution spectral curve in place of the real spectrum, readings of the filters may be calculated. It is found that the measured and the calculated readings do not agree, as they would if the low-resolution spectrum were equivalent to the real high-resolution spectrum in the production of filter readings. However, references 8 to 13 obtain such equivalence by applying corrections to the measured readings in such manner that the corrected spectral curve yields calculated readings equal to the measured readings. This corrected low-resolution spectrum is named the "filter equivalent spectrum" by reference 8. An "effective spread function" $g_E(\nu)$ associated with the equivalent spectrum method will be found, and it will be shown that the transforms of both the filter spread function and the interpolating function are compensated in the range $|s| < s_c$. Thereby, the averaging error is reduced.

The measured filter readings are a sequence of impulses that have a transform $\mathcal{N}^*(s)$ (ref. 16) which is periodic, with a period Λ, and is given by

$$\mathcal{N}^*(s) = \sum_{n=-\infty}^{\infty} \mathcal{N}\left[s + (n/\Lambda)\right]\mathcal{G}_e\left[s + (n/\Lambda)\right] \tag{33}$$

The equivalent spectrum is generated by fitting a curve through the corrected ordinates spaced at intervals Λ. Curve-fitting with an interpolating function $p(\nu)$ and the corrected ordinates $\overline{N}_E(\lambda_i)$ generates the equivalent spectrum

$$N_E(\lambda) = \sum_{i=-\infty}^{\infty} \overline{N}_E(\lambda_i)p(\nu) \tag{34}$$

The calculated filter readings are the result of integrating $N_E(\lambda) \cdot g_e(\nu)$ to produce readings $\overline{N}_E(\lambda_i)$. The samples are a sequence of impulses that have a transform like equation (33), given by

$$\mathcal{N}_E^*(s) = \sum_{n=-\infty}^{\infty} \mathcal{N}_E\left[s + (n/\Lambda)\right]\mathcal{G}_e\left[s + (n/\Lambda)\right] \tag{35}$$

The method of spectral curve compensation makes the filter readings equal to each other, and thus their transforms become equal, so that

$$\mathcal{N}_E^*(s) = \mathcal{N}^*(s) \tag{36}$$

If equations (33) and (35) are equated to each other, $\mathcal{G}_e(s)$ cannot be canceled if the terms of the summation overlap, which they generally do. In general, $\mathcal{N}_E(s) \neq \mathcal{N}(s)$.

The effective spread function for the equivalent spectrum method has a transform defined by

$$\mathcal{G}_E(s) \equiv \mathcal{N}_E(s)/\mathcal{N}(s), \quad |s| < s_c \tag{37}$$

In general, $\mathcal{G}_E(s) \neq 1$, because equations (33) to (36) are complex and asymmetrical. Furthermore, $\mathcal{G}_E(s)$ depends on the spectrum as well as on the filter spread function. However, an approximation of $\mathcal{G}_E(s)$ can be made, if the spectra $N(\lambda)$ and $N_E(\lambda)$ are sufficiently smooth curves, so that the terms in equations (33) and (35) do not significantly overlap. Then equation (37) becomes $\mathcal{G}_E(s) = 1$. Then the spread function $g_E(\nu) = \mathrm{sinc}(\pi\nu/\Lambda)$. Thus, the filter spread function $g_e(\nu)$ has been fully compensated in the range $|s| < s_c$. Since interpolation preceded the generation of $N_E(\lambda)$ and $\mathcal{N}_E^*(s)$ (eqs. (34) and (36)) and compensation followed the generation of these quantities, no separate compensation of the interpolating function is required.

The amount of compensation applied by this method must be limited by the proper choice of filter spacing ($\Lambda = 2\sigma$) so that the length C in figure 7 is not too small, as was discussed in the section Width and Spacing of Filters.

Example for a Filter Radiometer

The example used is the same as in the section Example of Averaging Error Reduction by Fourier-Transform Compensation. The Newton-Raphson method was used to adjust the original filter measurements to provide the filter equivalent spectrum and thereby to yield zero differences between the originally measured filter readings and the filter readings calculated for the filter equivalent spectrum. Fast convergence of the method was obtained by use of a tridiagonal Jacobian matrix, with the elements computed by numerical differentiation. Convergence was rapid because the size of the partial derivatives falls rapidly away from the principal diagonal. The subroutine of appendix B was used to solve the Jacobian system of equations.

The error is plotted in figure 13 for both linear and spline interpolation. The uncompensated values shown are the same as those shown in figures 10(a) and 11(a). With

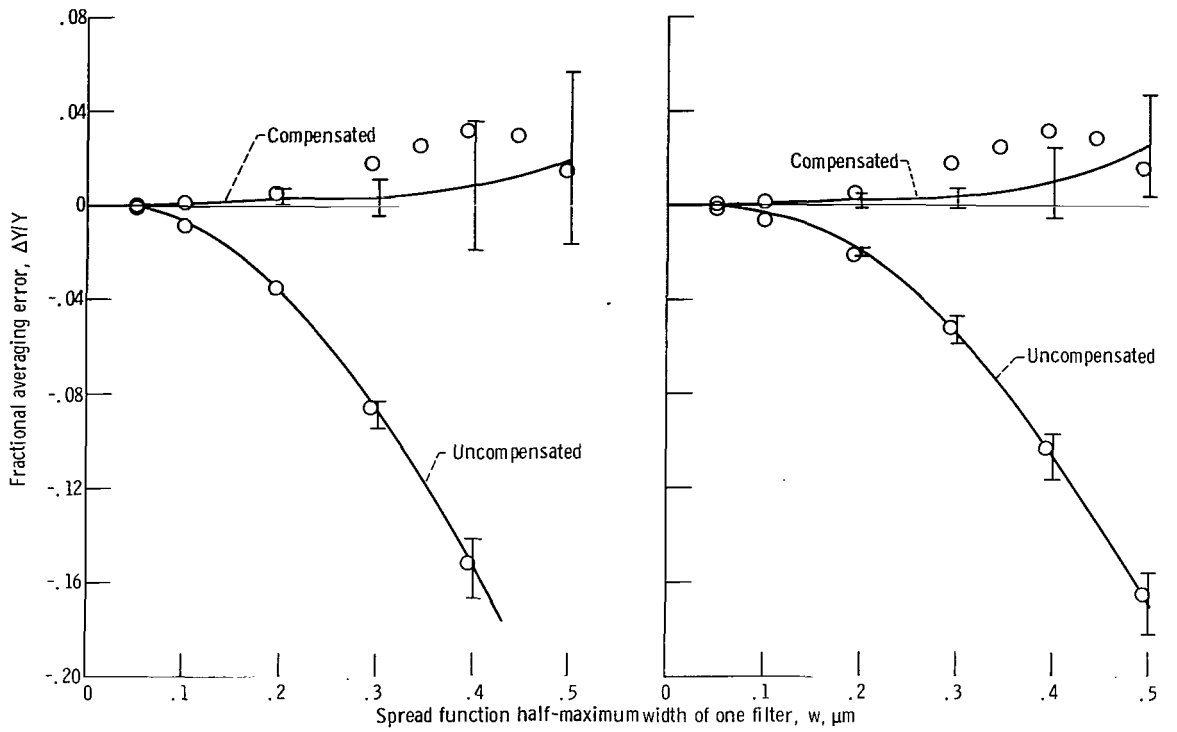

Figure 13. - Filter radiometer averaging error with spectral curve compensation. (Curves from eq. (12) (bars are average deviation); points from eq. (17), compensation with $g_E(\nu) = \mathrm{sinc}(\pi\nu/\Lambda)$, eq. (28).)

compensation, the points computed by equation (17) show overcompensation relative to the curve computed by equation (12) for $w > 0.2$ micrometer. Thus, the correct spread function for the equivalent spectrum probably lies between the function $\mathrm{sinc}(\pi\nu/\Lambda)$ and the spread functions in figures 10(b) and 11(b) for Fourier transform compensation.

Both systematic averaging error and random average deviation, after spectral-curve compensation, are less than the corresponding errors after Fourier transform compensation that are shown in figures 10(a) and 11(a). At 0.25 micrometer, a 3-percent systematic error was reduced to 0.3 percent, and the average deviation was 0.3 percent. Both linear and spline interpolation yield the same averaging error, but the average deviation is smaller with spline interpolation. Thus, the smallest errors are obtained with spline interpolation and spectral-curve compensation.

Figure 14 shows how the ordinates of the filter equivalent spectrum differ from those of the faired spectral curve drawn through the original measurements. The comparison is shown for both linear interpolation (fig. 14(a)) and cubic-spline interpolation (fig. 14(b)). A large negative value of the ordinate for the first filter, at $\lambda = 0.175$ micrometer, was required to generate the filter equivalent spectrum. As indicated in the

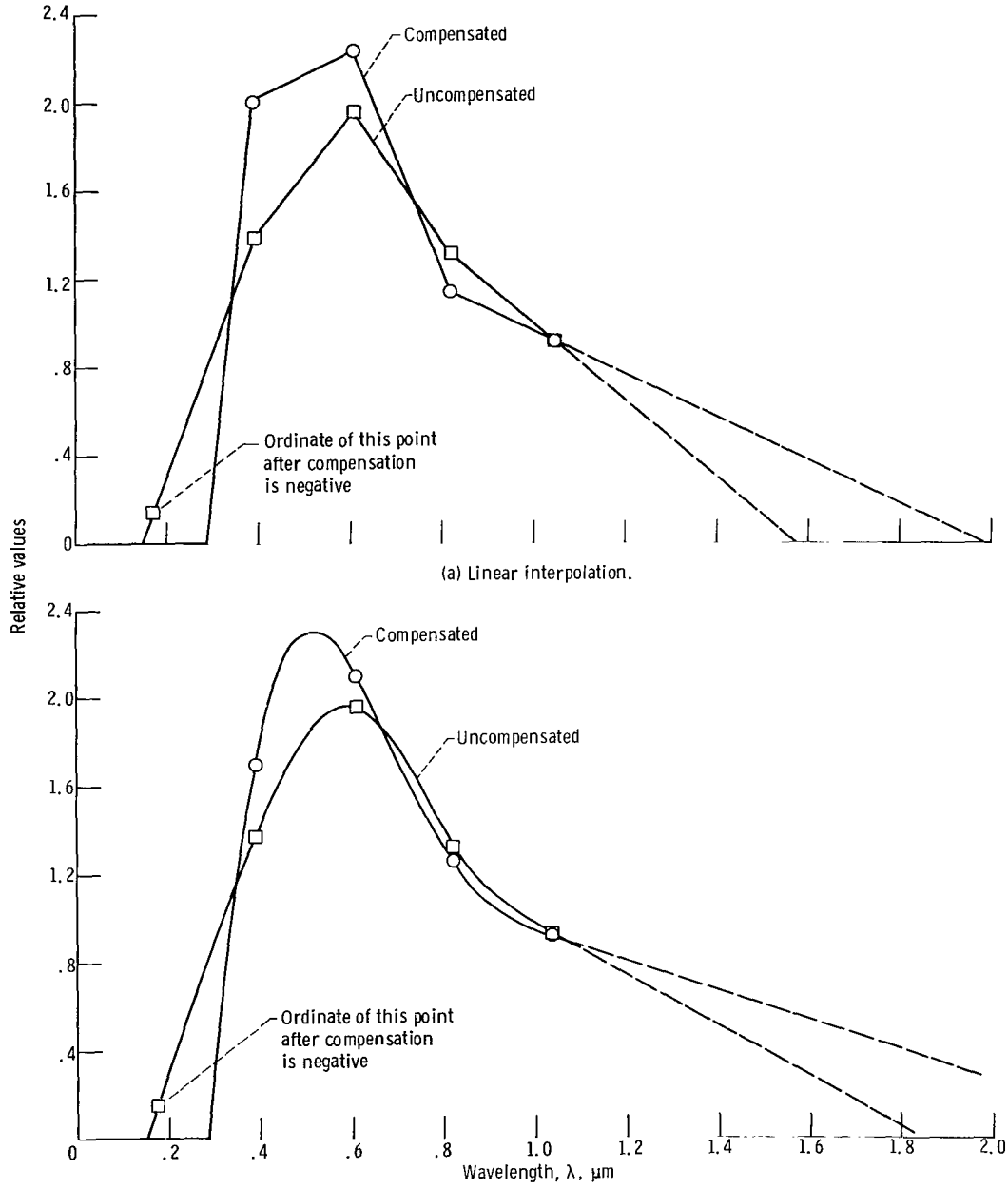

Figure 14. - Comparison of linear and spline interpolation with five filters of half-maximum width of 0.3 micrometer and xenon spectrum.

section Interpolation With a Finite Set of Unequally Spaced Filters, the negative values were replaced by zero before integrating the product of spectral radiation and the spread function.

SUMMARY OF RESULTS

An equation was derived for the error of a spectral average caused by low spectral resolution. In this equation, the spread function appeared explicitly so that the error could be related to the spread-function width. Error reduction by Fourier-transform compensation and by spectral-curve compensation was analyzed and examples were given. Both methods gave similar results. In an example of spectral-curve compensation, a systematic averaging error of 3 percent was reduced to 0.3 percent, with a random average deviation of 0.3 percent. Spectral-curve compensation is more adaptable than Fourier-transform compensation in those practical applications where the spread functions are not alike or are not equally spaced. Error reduction is also a useful approach to estimating the averaging error. The procedure is to find the value of the average before and after applying error reduction. Trial examples show that the error is less than the difference between these averages.

Spectroradiometers of the scanning type and the multiple-filter type were considered. Criteria were established for the optimum spacing of filters, having a given spread-function width, to minimize the errors. Recommendations were given for calculating the optimum location of the center wavelength of a filter and for interpolating between filter readings. An example showed that (1) spline interpolation produced a smaller averaging error than linear interpolation before averaging-error reduction was applied, (2) linear and spline interpolation produced substantially equal averaging errors after averaging-error reduction was applied, and (3) spline interpolation produced a smaller average deviation of the averaging error both before and after averaging-error reduction was applied.

The example also showed that, when a very small number of filters is used, there exists an optimum spread-function width that minimizes the averaging error or the overall error. In the particular example chosen, there was also little advantage to the use of more than four filters.

Thus, using the optimum filter-selection criteria and techniques of data analysis, small overall errors are achievable even when a small number of low-resolution filters is used.

Lewis Research Center,
National Aeronautics and Space Administration,
Cleveland, Ohio, September 29, 1970,
720-03.

APPENDIX A

SYMBOLS

A	normalizing constant, eq. (13)
a	constant of function $\mathscr{F}_C(s)$, eq. (22)
b	constant of function $\mathscr{F}_C(s)$, eq. (22)
C	amplitude of Fourier transform at $s = 1/(2\Lambda)$
d	filter spacing for spline interpolation, eq. (B2)
$\mathscr{F}$	Fourier transform of f
f	function to compensate g
$\mathscr{G}$	Fourier transform of g
g	spread function
h	cross correlation of N and g, eq. (15)
N	infinite resolution spectrum
$\mathscr{N}$	Fourier transform of N
$\mathscr{P}$	Fourier transform of p
p	interpolating function
s	abscissa of Fourier transform
u	variable for spline interpolation
w	half-maximum width of spread function
Y	weighted average of y
ΔY	error in Y
y	response function
z	variable for spline interpolation
Λ	separation of filter center wavelengths
λ	wavelength
λ_i	nominal center wavelength of a filter, or wavelength setting of a spectrometer
ν	wavelength auxiliary variable, $\nu = \lambda - \lambda_i$
σ	standard deviation of spread function, eq. (24)
τ	transmission factor, or function $\tau(\nu)$

Subscripts:

C compensated

c sampling cutoff

E equivalent spectrum

e even spread function

f set of filters

o odd function

p interpolating function

0 reference value

Superscripts:

$\bar{}$ associated with low resolution

* Fourier transform of a sequence of impulses

APPENDIX B

CUBIC-SPLINE INTERPOLATION

The cubic spline is a cubic polynomial between each pair of ordinates, which also has a continuous second derivative that varies linearly between each pair of ordinates. It is computed within each interval between filter readings $\overline{N}_i$ and $\overline{N}_{i+1}$ at center wavelengths λ_i and λ_{i+1} by the equation

$$\overline{N}(\lambda) = \left[(\lambda - \lambda_i)\overline{N}_{i+1} + (\lambda_{i+1} - \lambda)\overline{N}_i\right]\Big/d_i$$

$$- (\lambda - \lambda_i)(\lambda_{i+1} - \lambda)\left[(d_i + \lambda_{i+1} - \lambda)u_i + (d_i + \lambda - \lambda_i)u_{i+1}\right]\Big/6d_i \qquad \begin{cases}\lambda_i \le \lambda \le \lambda_{i+1} \\ i = 1, \ldots, n-1\end{cases} \tag{B1}$$

The computation is made for n filters with spacings

$$\left.\begin{aligned} d_i &= \lambda_{i+1} - \lambda_i \\ i &= 1, \ldots, n-1 \end{aligned}\right\} \tag{B2}$$

The second derivatives u_i of the spline are the solution of the system of equations

$$\begin{bmatrix} B_2 & C_2 & 0 & 0 \\ A_3 & B_3 & C_3 & 0 \\ 0 & \cdots & \cdots & \cdots \\ 0 & 0 & A_{n-1} & B_{n-1} \end{bmatrix} \begin{bmatrix} u_2 \\ u_3 \\ \cdots \\ u_{n-1} \end{bmatrix} = \begin{bmatrix} z_2 \\ z_3 \\ \cdots \\ z_{n-1} \end{bmatrix} \tag{B3}$$

with $u_1 = u_n = 0$ and

$$z_i = 6(\overline{N}_{i+1} - \overline{N}_i)/d_i - 6(\overline{N}_i - \overline{N}_{i-1})/d_{i-1} \qquad i = 2, \ldots, n-1 \tag{B4}$$

The three diagonals of the matrix are

$$\left.\begin{aligned} A_i &= d_{i-1} \\ B_i &= 2(d_{i-1} + d_i) \\ C_i &= d_i \end{aligned}\right\} \quad i = 2, \ldots, n-1$$

An efficient method for the solution of a tridiagonal system like equation (B3) is given by reference 22. The solution is concisely expressed as the following FORTRAN IV subroutine:

```
      SUBROUTINE SIMEQ (N,A,U)
C     SOLVES TRIDIAGONAL N BY N MATRIX, MAIN DIAGONAL A(2,I),I=1,N, LOWER DIAGONAL
C     A(1,I),I=2,N , UPPER DIAGONAL A(3,I),I=1,N-1 , RIGHT SIDE A(4,I),I=1,N),
C     SOLUTION U(I),I=1,N, STORAGE A(5,I),A(6,I),I=1,N
      DIMENSION A(6,N), U(N)
      A(6,1)= A(2,1)
      DO 10 I=2,N
      A(5,I)= A(1,I)/A(6,I-1)
   10 A(6,I)=A(2,I)-A(5,I)*A(3,I-1)
      U(1)=A(4,1)
      DO 11 I=2,N
   11 U(I)=A(4,I)- A(5,I)*U(I-1)
      U(N)= U(N)/A(6,N)
      DO 13 J=2,N
      I= N-J+1
   13 U(I)=(U(I)-A(3,I)*U(I+1))/A(6,I)
      RETURN
      END
```

To solve equation (B3) for u_i using equation (B4), let $N = n - 2$ and

$$U(I) = u_{i+1}$$

$$A(1, I) = d_i$$

$$A(2, I) = 2(d_i + d_{i+1})$$

$$A(3, I) = d_{i+1}$$

$$A(4, I) = z_{i+1}$$

where $I = i = 1, \ldots, n - 2$.

REFERENCES

1. Curtis, Henry B.: Effect of Error in Spectral Measurements of Solar Simulators on Surface Response. NASA TN D-5904, 1970.

2. Hardy, Arthur C.; and Young, F. Mansfield: The Correction of Slit-Width Errors. J. Opt. Soc. Am., vol. 39, no. 4, Apr. 1949, pp. 265-270.

3. Bracewell, Ronald N.: Simple Graphical Method of Correcting for Instrumental Broadening. J. Opt. Soc. Am., vol. 45, no. 10, Oct. 1955, pp. 873-876.

4. Jones, Robert A.; and Coughlin, John F.: Elimination of Microdensitometer Degradation from Scans of Photographic Images. Appl. Opt., vol. 5, no. 9, Sept. 1966, pp. 1411-1414.

5. Shack, Roland V.; and Swindell, William: An Analog Image Processor. Evaluation of Motion-Degraded Images. NASA SP-193, 1969, pp. 175-178.

6. Horner, Joseph L.: Optical Restoration Using Optimum Filter Theory of Images Blurred by Atmospheric Turbulence. Evaluation of Motion-Degraded Images. NASA SP-193, 1969, pp. 105-111.

7. Harris, James L., Sr.: Potential and Limitations of Techniques for Processing Linear Motion-Degraded Imagery. Evaluation of Motion-Degraded Images. NASA SP-193, 1969, pp. 131-138.

8. Wagoner, Ralph E.; and Pollack, John L.: Data Reduction for Filter Spectroradiometry. NASA TN D-3037, 1965.

9. Moran, Hubert S.: Determination of the Relative Spectral Sensitivity of Phototubes. J. Opt. Soc. Am., vol. 45, no. 1, Jan. 1955, pp. 12-14.

10. Wyszecki, Günter: Multifilter Method for Determining Relative Spectral Sensitivity Functions of Photoelectric Detectors. J. Opt. Soc. Am., vol. 50, no. 10, Oct. 1960, pp. 992-998.

11. Mori, N.: Spectral Sensitivity Determinations by Cutoff Filters. J. Opt. Soc. Am., vol. 51, no. 9, Sept. 1961, pp. 1015-1023.

12. Jansson, Peter A.; Hunt, Robert H.; and Plyler, Earle K.: Resolution Enhancement of Spectra. J. Opt. Soc. Am., vol. 60, no. 5, May 1970, pp. 596-599.

13. Jansson, Peter A.: Method for Determining the Response Function of a High-Resolution Infrared Spectrometer. J. Opt. Soc. Am., vol. 60, no. 2, Feb. 1970, pp. 184-191.

14. Bracewell, Ronald N.: The Fourier Transform and Its Applications. McGraw-Hill Book Co., Inc., 1965.

15. Quittner, G.: On Error Propagation in the Resolution Correction. Nucl. Inst. Meth., vol. 39, 1966, pp. 271-277.

16. Papoulis, Athanasios: The Fourier Integral and Its Applications. McGraw-Hill Book Co., Inc., 1962.

17. Helms, H. D.; and Thomas, J. B.: Truncation Error of Sampling-Theorem Expansions. Proc. IRE, vol. 50, no. 2, Feb. 1962, pp. 179-184.

18. Simpson, R. S.; and Salter, W. E.: A Tighter Bound on Sampling Error for the Cardinal Series. Proc. IEEE, vol. 54, no. 8, Aug. 1966, pp. 1066-1067.

19. Haber, F.: Rapidly Converging Sample Weighting Functions. IEEE Trans. on Comm. Syst., vol. CS-12, no. 1, Mar. 1964, pp. 116-117.

20. Lerner, R. M.: Representation of Signals. Lectures on Communication System Theory. Elie J. Baghdady, ed., McGraw-Hill Book Co., Inc., 1961, ch. 10.

21. Handscomb, David C., ed.: Methods of Numerical Approximation. Pergamon Press, 1966, ch. 19.

22. Forsythe, George E.; and Moler, Cleve B.: Computer Solution of Linear Algebraic Systems. Prentice-Hall, Inc., 1967.

NASA-Langley, 1971 —— 14 E-5271

NATIONAL AERONAUTICS AND SPACE ADMINISTRATION
WASHINGTON, D.C. 20546
OFFICIAL BUSINESS

FIRST CLASS MAIL

POSTAGE AND FEES PAID
NATIONAL AERONAUTICS AN
SPACE ADMINISTRATION

"The aeronautical and space activities of the United States shall be conducted so as to contribute . . . to the expansion of human knowledge of phenomena in the atmosphere and space. The Administration shall provide for the widest practicable and appropriate dissemination of information concerning its activities and the results thereof."

—NATIONAL AERONAUTICS AND SPACE ACT OF 1958

NASA SCIENTIFIC AND TECHNICAL PUBLICATIONS

TECHNICAL REPORTS: Scientific and technical information considered important, complete, and a lasting contribution to existing knowledge.

TECHNICAL NOTES: Information less broad in scope but nevertheless of importance as a contribution to existing knowledge.

TECHNICAL MEMORANDUMS: Information receiving limited distribution because of preliminary data, security classification, or other reasons.

CONTRACTOR REPORTS: Scientific and technical information generated under a NASA contract or grant and considered an important contribution to existing knowledge.

TECHNICAL TRANSLATIONS: Information published in a foreign language considered to merit NASA distribution in English.

SPECIAL PUBLICATIONS: Information derived from or of value to NASA activities. Publications include conference proceedings, monographs, data compilations, handbooks, sourcebooks, and special bibliographies.

TECHNOLOGY UTILIZATION PUBLICATIONS: Information on technology used by NASA that may be of particular interest in commercial and other non-aerospace applications. Publications include Tech Briefs, Technology Utilization Reports and Technology Surveys.

Details on the availability of these publications may be obtained from:

SCIENTIFIC AND TECHNICAL INFORMATION OFFICE

NATIONAL AERONAUTICS AND SPACE ADMINISTRATION

Washington, D.C. 20546